Photochemistry of K-590 in the Room-Temperature Bacteriorhodopsin Photocycle†

J. K. Delaney,‡ P. K. Schmidt,‡ T. L. Brack,§ and G. H. Atkinson*,‡

Department of Chemistry and Optical Science Center, University of Arizona, Tucson, Arizona 85721, and Department of Chemistry, Hofstra University, Hempstead, New York 11549

Received: January 31, 2000; In Final Form: May 11, 2000

The photochemistry of the K-590 intermediate in the room-temperature (RT) bacteriorhodopsin (BR) photocycle (i.e., K-590 back reaction) is examined with picosecond time resolution over the 50 ps to 4.5 ns period of its lifetime. Three separate, 4−5-ps (fwhm) pulses are used at different wavelengths to sequentially (i) initiate the BR photocycle by optical excitation of BR-570 (pump 1 at 578 nm), (ii) photolytically interrupt the RT/BR photocycle at selected time delays between 50 ps and 4.5 ns after BR-570 excitation (pump 2 at 650−660 nm), and (iii) monitor the changes in sample absorbance after BR-570 or BR-570 and K-590 excitation (probe at 570−620 nm). The wavelengths of these laser pulses are selected to optimize their respective functions in terms of photolysis or monitoring changes in absorbance. The timing relationships between the pump 1, pump 2, and probe pulses, all with independently controlled pulse widths, energies, and wavelengths, are selected to obtain two different types of pulse sequences: (i) a two-pulse timing sequence designed to monitor intermediate concentrations in the forward, uninterrupted BR photocycle and (ii) two different, three-pulse timing sequences designed to characterize the optically induced, picosecond RT/K-590 photochemistry (back reaction). The results show that (i) the species formed by the 650−660-nm excitation of K-590 can be identified via its absorption spectrum as BR-570, (ii) BR-570 is formed from K-590 within the 5-ps cross-correlation time defined by the pump 2 and probe pulses, (iii) the K-590 to BR-570 mechanism does not appear to involve an intermediate analogous to J-625 found in the forward BR photocycle, and (iv) the spectroscopic characteristics of the K-590 back reaction remain unchanged for pump 2 delays of 100 ps to 4.5 ns, indicating that the K-590 photochemistry (i.e., relative quantum efficiency and photoproduct) remains constant over this time interval. These results are discussed with respect to previous studies of the K-590 back reaction (i) at low temperatures and (ii) at RT using high-power, nanosecond pulsed excitation both of which create photostationary mixtures of intermediates. The mechanistic interpretation of these picosecond, RT results, including the relationship(s) to the forward BR photocycle, derives from structural changes in the retinal chromophore and its protein binding pocket, as well as their respective interactions.

Introduction

The biochemistry of the *trans*-membrane protein bacteriorhodopsin (BR) found in the purple membrane of *Halobacterium salinarium* has been shown to involve a novel proton-pumping mechanism that derives from high-efficiency energy storage and signal transduction processes.[1−3] Specifically, the light-driven proton pump in BR functions to produce an electrochemical gradient across the purple membrane. The resultant chemical gradient is utilized for proton translocation and ATP synthesis.[2] BR is unusually accessible to spectroscopic measurements because it cycles back to its original state (BR-570) within about 5−10 ms after optical excitation via a series of transformations in the retinal chromophore structure and protein/retinal interactions, thereby defining the BR photocycle at room temperature (RT). The RT/BR photocycle has also been widely identified as a model for the related processes in the RT rhodopsin photoreaction, which underlies visual processes in vertebrates and many invertebrates.[4,5]

In light-adapted samples, the BR photocycle is initiated by optical excitation but subsequently is composed of a sequential series of ground electronic state reactions.[2,6] The molecular dynamics underlying the early stages of the RT/BR photocycle have been examined extensively using transient electronic absorption spectroscopy[7−10] and time-resolved vibrational spectroscopy, including Raman (spontaneous and coherent) scattering[11−17] and infrared absorption.[18−23] These spectroscopic studies have shown that intermediates in the BR photocycle reflect sequential structural (configurational and conformational) changes in both the retinal chromophore and the protein environment that surrounds it, and as a consequence, alterations in the steric and electrostatic interaction(s) between particular regions of the retinal chromophore and specific amino acid moieties.[7−23]

In addition to the forward, ground-state reaction pathway known as the RT/BR photocycle, optically induced back reactions originating from photocycle intermediates have been identified.[24−31] These photolytic back reactions effectively interrupt the BR photocycle at a given time in its evolution by converting at least one intermediate into another species, widely presumed to be BR-570. Such a photolytic interruption is not part of the normal RT/BR photocycle nor is it derived from any of the thermal equilibria established between ground-state intermediates constituting the RT/BR photocycle.[32] The identity of the back reaction photoproduct(s), as well as the molecular mechanism(s) underlying a specific back reaction, remains largely to be established, especially at RT.

† Part of the special issue "Thomas Spiro Festschrift".
* Author to whom correspondence should be addressed.
‡ University of Arizona.
§ Hofstra University.

10.1021/jp000374e CCC: $19.00
Published on Web 08/01/2000

The spectroscopic and kinetic characterization of these back reactions also provides new insight into the mechanism of the forward BR photocycle, especially with respect to the time-dependent changes in the structures of and interactions between the retinal chromophore and protein environment that constitute the photocycle. These changes can be envisioned in terms of a mechanistic clock that reflects the simultaneous and interdependent changes in both the retinal and its protein environment. A variety of examples of the correlation between retinal and its protein have been identified in the BR photocycle: Trp182/retinal interaction upon the formation of K-590,[33] tilting of the F/G helices during the M-420 lifetime,[34] the protonation state of Asp96 during the formation and decay of M-420,[35,36] etc. Photolytic interruption at a given time after the BR photocycle is initiated, therefore, samples a specific set of structures (retinal and protein) and interactions that define the mechanistic clock and that determine the specificity and efficiency of the forward BR photocycle. Given the importance of these molecular parameters in the forward BR photocycle, it is reasonable to anticipate that they also control the photolytically induced back reactions.

Much of the work on BR back reactions, and especially on the K-590 back reaction, has been performed at low temperatures (LT) selected to trap specific BR photocycle intermediates.[24,25,29,31,36−43] There is no *a priori* reason, however, why such a LT sample should be homogeneous. Previous studies[29,31] have shown that multiple species are present at LT, resulting in heterogeneous BR samples, *vide infra*. Irradiation of the mixture of BR species trapped at LT has been shown to result in photochemistry (i.e., reformation of BR-570 from M-412[44,45] and from K-590[46−49]). These LT experiments use steady-state illumination to alter the photostationary state mixture of species created by thermal trapping. Thus, these studies primarily focus on establishing the existence of back reactions and not on elucidating the mechanistic pathway by which they proceed.

Furthermore, because the retinal/protein structures and interactions underlying the RT/BR photocycle mechanism are anticipated to be temperature-dependent, the relationship(s) between the LT and RT mechanisms remains open to interpretation. Although the K-590 to BR-570 back reaction has also been studied at RT, the experimental conditions used have perpetuated some of the limitations found in the LT work, namely, photochemical data from photostationary-state mixtures of BR species. These RT experiments have been conducted using both (i) ∼10-ns, pulsed excitation from a single laser with sufficiently high energies to create photostationary-state mixtures of K-590 and BR-570[24,28] and (ii) ∼10-ns, time-resolved, pulsed excitation from two independently controlled lasers with probe energies selected to be provide minimal perturbation in the photocycle.[30] The first of these studies extracted information on the relative yield of the K-590 to BR-570 transformation, whereas the latter study obtained the wavelength and power (probe pulse at a 10-ns time delay) dependence for the K-590 to BR-570 transformation. Given the picosecond time scale for the processes involved (e.g., the excited electronic state lifetime of K*-590 and the time anticipated for C═C isomerization itself), a detailed elucidation of the K-590 to BR-570 back reaction requires picosecond time resolution and an experimental procedure that can distinguish the K-590 photochemistry from that of the RT/BR photocycle.

The properties of K*-590 have independently been examined in several studies. Measurements of picosecond time-resolved fluorescence spectra show that, although the fluorescence yields from K*-590 and BR*-570 are comparable, their respective fluorescence spectra are readily distinguishable.[50−52] A recent study of the excited-state mechanism in the BR photocycle concluded that the lifetime of K*-590 is about 100 fs.[52,53]

In this paper, picosecond time resolution and probe wavelengths over the 560−660-nm region are used to characterize the RT/K-590 back-reaction mechanism and to identify its photoproduct. These experiments utilize three, independently controlled, picosecond (4−5 ps, fwhm) laser pulses to sequentially (i) initiate the BR photocycle by optically exciting BR-570 (pump 1 at 578 nm); (ii) excite the BR photocycle mixture present at a fixed time delay between 50 ps and 4.5 ns after BR-570 excitation, thereby initiating the K-590 photochemistry (pump 2 at 650−660 nm); and (iii) monitor the picosecond transient absorption (PTA) in the sample 4.0−4.5 ns after BR-570 excitation (probe at 570−620 nm). This examination seeks not only to elucidate K-590 photochemistry, but also to reveal the role(s) of structural changes in the retinal, the protein, and/or in their respective interactions that are required to facilitate specific reactive pathways (e.g., C_{13}═C_{14} isomerization) in the RT/BR photocycle.

Experimental Section

1. Sample Preparation. The BR purple membrane (strain S-9) is prepared using published procedures.[54] The purity of the sample, dissolved as a suspension in doubly distilled water (pH = 6.6 before and after PTA experiments), is confirmed by an absorbance (A) ratio defined as A_{280nm}(protein)/A_{570nm}(retinal) < 1.8.

2. Instrumentation. The instrumentation utilized for these experiments is similar to that described elsewhere,[52] but the specific configurations of the pulse sequences used require some discussion. The laser instrumentation consists of three mode-locked, cavity-dumped dye lasers (Coherent, model 701−1, cavity dumper system 7200/7220), each operating at a 1-MHz repetition rate. All three dye lasers are synchronously pumped by the frequency-doubled output (∼650 mW at 527 nm) of a mode-locked Nd:YLF laser (Coherent, model Antares 76), which is operated at 76 MHz. The 527-nm radiation is distributed between the three dye lasers [operated with Rhodamine 590 for 578 nm (pump 1) and 570−620 nm (probe) and Kiton Red for 650−660 nm (pump 2)] using polarizer/half-wave plate combinations that collectively act as variable beam splitters. All three dye lasers use a one-plate birefringent filter to obtain a spectral bandwidth of 1 nm (fwhm).

The conversion from 76-MHz pumping to 1-MHz dye laser operation is achieved through a cavity dumper. The suppression ratio (intensity of selected pulse/intensity of each of the two temporally adjacent pulses) is >1:20 in the dye laser (at 1 MHz).

Under these pumping conditions, the output of each dye laser is ∼40 nJ/pulse, with an autocorrelation width of 4.5 ps at a 1-MHz repetition rate. The adjustment of the output powers from the dye lasers used for pump 1 and pump 2 depends on the type of measurement: (i) for power-dependent data, the RF power on the Bragg cell in the cavity dumper is adjusted, and (ii) for kinetic data, the polarizer/half-wave plate combinations in the output beams are adjusted. The output power of the probe laser is controlled by adjusting a Glan−Thompson prism located in its beam path, thereby ensuring wavelength-independent power attenuation.

The timing between the three dye laser pulses is determined by three, independently controlled optical delay lines and a series of beam-expansion optics. The dye laser outputs pass through beam-expanding optics (i.e., Galilean telescopes) that magnify (×5) the beam diameter to 3 mm, thereby reducing the beam

divergence prior to its entry into the delay line. Time delays of up to 5 ns are accessible with the optical delay lines operated with these telescopes. The delay lines consist of corner-cube reflectors (trihedral prisms with a tolerance of 3 arc s) mounted on 90-cm mechanical translation stages. Stepping motors are operated under computer control to adjust the position of the prisms to minimize spatial deviations (±5%) introduced by moving the delay lines. One revolution consists of 200 steps, which results in a 5-μm minimum step size.

Pellicles (5-μm thickness), used to avoid secondary reflections from two surfaces, combine the three laser beams after each exits a delay line. A coated pellicle combines the beams from pump 1 and pump 2 lasers, while an uncoated pellicle combines these two pump beams with that from the probe laser. The appropriate combinations of pump and probe beams are directed to an autocorrelator (Femtochrome, model FR-103XL) for the measurement of auto- and cross-correlation times (CCT). The timing jitter between the dye laser pulses and the pulse-to-pulse power stability are both optimized prior to each experiment. The precise values of zero time and the CCT for each scan are measured in a separate PTA trace recorded in parallel with the PTA data presented here.

These combinations of laser beams are focused with a microscope objective into a 350 ± 10 μm (diameter) flowing, liquid jet of the BR−water suspension. The jet is created by mechanical pumping of the BR−water suspension through a cylindical glass nozzle. The reservoir containing the BR−water suspension is immersed, together with the pump head, in an ice−water bath in order to maintain the sample temperature at ∼10 °C in the jet. The 100 mL/min flow rate ensures that the liquid jet has a speed of ∼17 m/s at the focal spot (∼10 μm diameter). These focusing and flow conditions, together with the laser repetition rates, ensure that the BR sample volume is fully exchanged between sets of laser pulses. This conclusion is confirmed by PTA measurements made at long time delays (electronically scanned from 100 ps to 600 ns) when the effects of the sample volume being partially exchanged within the focal volume can be observed.

The beams exiting the sample are recollimated before being dispersed by an 1800 line/mm, holographic grating in order to separate the probe beam from the pump beam(s). Beam steering is used to ensure that p-polarized light is incident on the grating in order to optimize its efficiency. The probe beam is detected by a photodiode−amplifier hybrid (EG&G HB2000). Since the intensity variation between probe pulses due to absorbance changes in the sample are small (10^{-3} OD), a phase-sensitive, lock-in amplifier (EG&G PARC, model 5101) is used to increase the signal-to-noise ratio. A mechanical chopper intersecting both pump beams modulates the probe signal at either 340 or 920 Hz. The DC output of the lock-in amplifier is transferred to a computer utilizing an A/D acquisition board.

3. Experimental Procedure. The timing sequences by which the three picosecond laser pulses (pump 1, pump 2, and probe) are used to examine the RT/K-590 photochemistry are represented schematically in Figure 1, together with the more conventional two-pulse sequence (PTA) used to monitor the time evolution of BR photocycle intermediates. In the latter case, the time between the pump 1 and probe pulses is continuously varied (via a scanning delay line) from negative values (i.e., probe pulse arriving at the sample jet prior to the pump 1 pulse) to positive values as large as 5.0 ns (Figure 1A). Two different experiments are performed using three-pulse timing sequences: (i) the time between pump 1 and the probe pulses is varied from negative values to delays as long as 4.5 ns while

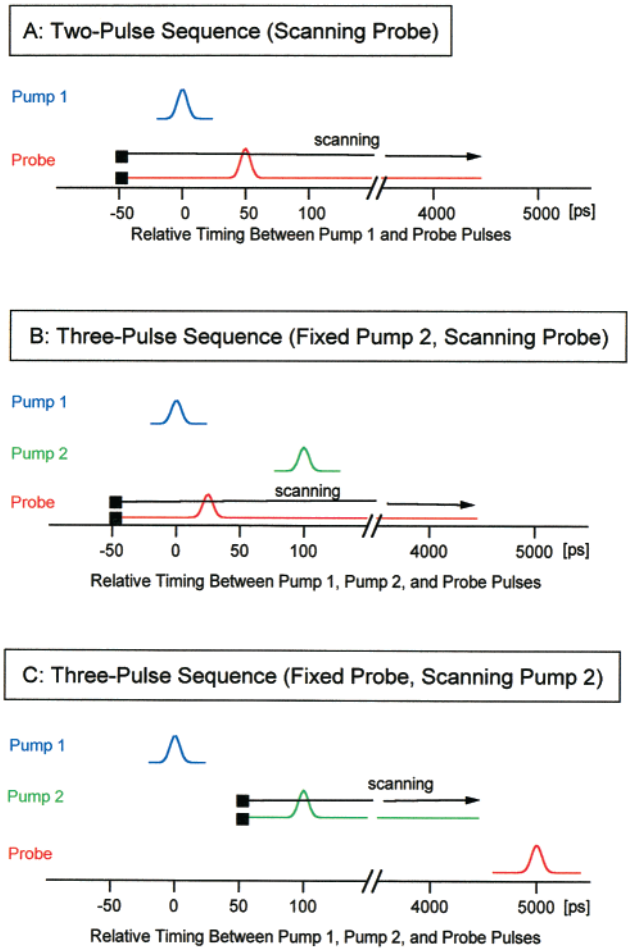

Figure 1. Picosecond pulse sequences used in the three types of experiments designed to investigate the time scale and mechanism(s) describing the K-590 back-reaction. (A) Two-pulse sequence designed to monitor the picosecond transient absorption (PTA) that can be assigned to the intermediates formed following the photolytic initiation of the room-temperature (RT) BR photocycle. PTA data identifying J-625 and K-590 are recorded (Figure 3). Pump 1 [4 ps (fwhm) at 578 nm] excites ground-state BR-570 to initiate the photocycle, while the probe pulse [4 ps (fwhm) between 560 and 660 nm] monitors changes in sample absorbance (ΔA). (B) Three-pulse sequence designed to initiate K-590 photochemistry. A second pump pulse [pump 2, 5 ps (fwhm) at 660 nm] is used to excite the BR-570 and K-590 mixture present 100 ps after the initiation of the photocycle by pump 1. The probe pulse [5 ps (fwhm) between 570 and 620 nm] is temporally scanned from −50 ps (prior to pump 1) to 4.5 ns after pump 1 to monitor the K-590 population. (C) Three-pulse sequence designed to determine if K-590 photochemistry changes during the 50 ps to 4.5 ns period of its lifetime. With the probe pulse delay fixed at 4.5 ns, the time delay between pump 1 and pump 2 is varied from 50 ps to 4.5 ns. Variations in the K-590 photochemistry can be detected from changes in ΔA values monitored by the probe pulse.

the pump 2 pulse delay (relative to pump 1) is fixed at 100 ps (Figure 1B) and (ii) the time between the pump 1 and pump 2 pulses is varied from negative values to delays as long as 4.5 ns while the probe pulse delay (relative to pump 1) is fixed at 4.5 ns (Figure 1C). In both cases, pump 1 is used to partially convert BR-570 into a transient mixture of intermediates. Because the shortest time delay between pump 1 and pump 2 is 100 ps, the sample population examined is distributed between only BR-570 and K-590. This conclusion is based on the widely accepted kinetic model describing the forward BR photocycle during this time interval (Figure 2).

The relative populations of these BR species, as predicted by this kinetic model, are shown schematically in Figure 2,

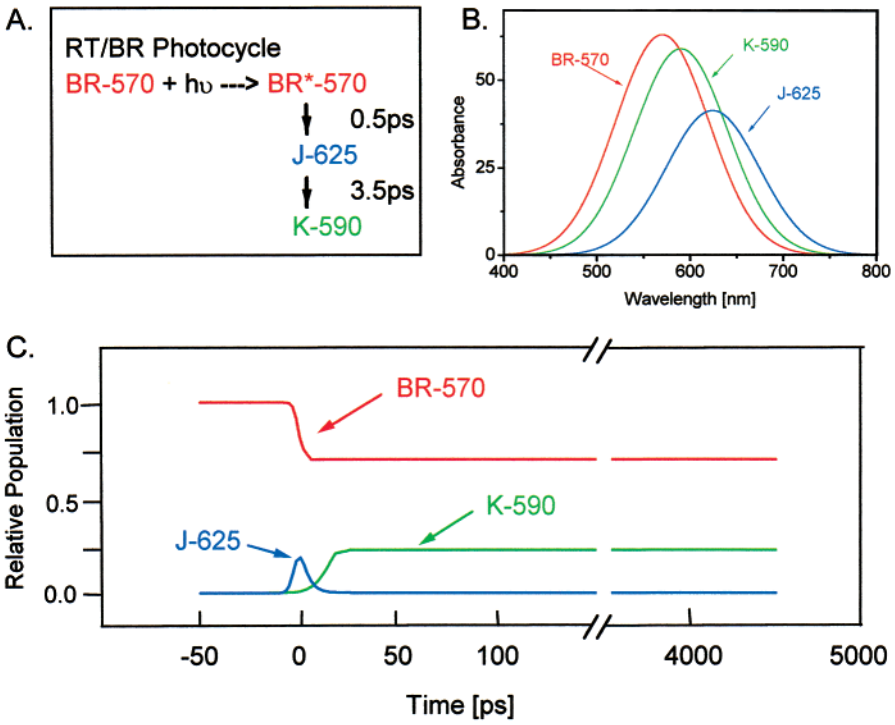

Figure 2. (A) Kinetic model describing the initial 5 ps of the RT/BR photocycle involving BR-570, J-625, and K-590.[52] (B) Schematic representation of the absorption spectra that can be assigned to BR-570, J-625, and K-590. An isobestic point between BR-570 and K-590 appears at 589 nm. (C) Approximate time-dependent concentrations of BR-570, J-625, and K-590 during the initial 5 ns of the RT/BR photocycle. These transient populations both are consistent with the kinetic model (A) and are derived from PTA data recorded using a two-pulse sequence such as that described in Figure 1A (i.e., pump 1 causes the depletion of the BR-570 population and leads to the formation of J-625 and K-590).

together with the absorption spectra of BR-570, K-590, and J-625. Pump 2 (650−660-nm) is utilized here to preferentially excite K-590 to K*-590, although absorption by BR-570 does occur to a small degree. Low-intensity probe pulses are used to monitor changes in the sample absorbance without photolytically altering the sample population to a significant degree. The wavelength of the probe pulses is varied for each type of pulse sequence to spectroscopically characterize the photoproduct(s) formed by K-590 excitation.

Results

The picosecond laser pulse sequences used in these experiments (Figure 1) are designed primarily to monitor three different, but related types of absorbance changes (ΔA) in a BR sample occurring in the pico/nanosecond time regime. These pulse sequences are used to examine the BR sample under the same experimental conditions and specifically involve (i) a two-pulse sequence (Figure 1A) to monitor conventional PTA for the formation of J-625 and its transformation to K-590 with <5-ps time resolution, (ii) a three-pulse sequence (Figure 1B) to determine the absorption spectrum of the photoproduct formed by the 660-nm (5 ps) excitation of K-590, and (iii) a three-pulse sequence (Figure 1C) to determine whether the photochemistry of K-590 changes over the 50 ps to 4.5 ns interval of its lifetime. Collectively, these data are used to quantitatively characterize the RT/K-590 back reaction over the 50 ps to 4.5 ns time interval of the RT/BR photocycle.

1. BR-570 → K-590 Forward Reaction. The processes that make up the initial 100 ps of the RT/BR photocycle have been determined from PTA measurements[7,52] of the type reproduced here by the two-pulse sequence (Figure 1A). These PTA data lead to a model for the transient populations of the J-625 and K-590 intermediates and the time-dependent depletion of the ground-state BR-570 that is shown schematically in Figure 2. The broad, overlapping absorption spectra of BR-570, J-625, and K-590 (Figure 2) ensure that the transient populations of more than one species are normally observed at a given probe wavelength. This point is illustrated by the PTA data observed with a two-pulse sequence for three different probe wavelengths used to monitor the initial 100 ps of the BR photocycle (Figure 3) following the 4.5-ps (fwhm) excitation of BR-570 at 578 nm (pump 1). For example, the appearance and decay of J-625 is observed at 620 nm, followed by the formation of K-590, the concentration of which remains constant over the 30−100-ps interval shown in Figure 3, prior to the arrival of another laser pulse (i.e., pump 2, *vide infra*). If the BR sample remains unperturbed by subsequent light excitation (e.g., pump 2), the K-590 population remains constant for delays of at least 4.5 ns.[16,22,56] Only the initial 100-ps interval of the unperturbed RT/BR photocycle is reproduced in Figure 3. Other probe wavelengths (e.g., 589 and 570 nm) detect only the recovery of the BR-570 population and/or the appearance of K-590. At all of these wavelengths, the J-625 transient population still influences the kinetics derived from the PTA data, even though absorption that can be assigned directly to J-625 is not observed in the data described here (Figure 3, <100 ps).

These PTA data also reveal a 589-nm isobestic point (Figure 3, <100 ps) at which BR-570 and K-590 have equal absorption coefficients. The existence of the 589-nm isobestic point supports the conclusion that only BR-570 and K-590 are present in the sample at 30 ps (i.e., J-625 has disappeared). The amount of K-590 present at 30 ps can be estimated to be ∼20% of the initial BR-570 concentration [taken from the measured BR-570 concentration, the K-590 absorption coefficient, and the measured ΔA (Figure 3)]. Because the two-pulse, 589-nm PTA data (not shown) exhibit no changes in ΔA over the 50 ps to 5 ns interval, the K-590 concentration remains constant throughout

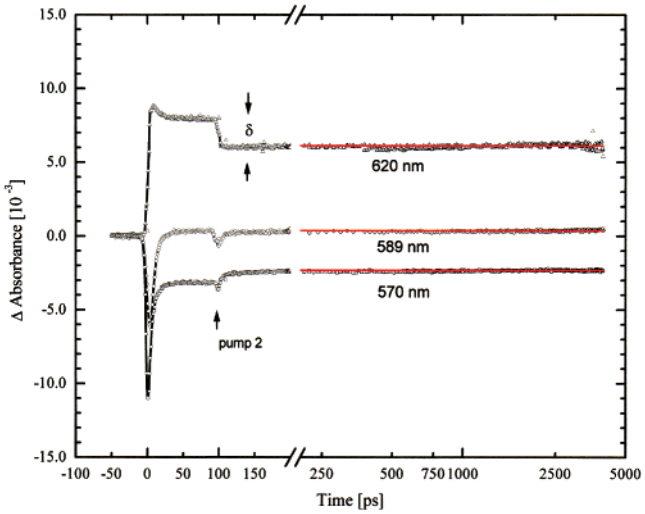

Figure 3. PTA traces measured using the three-pulse sequences described in Figure 1A (−50 to 100 ps) and Figure 1B (following the appearance of pump 2, between 100 ps and 5 ns after pump 1). PTA data for −50 to 100 ps show the appearance of J-625 and K-590, while the PTA data recorded after the appearance of pump 2 are analyzed in terms of the K-590 back reaction (see text). The absence of long-term changes in ΔA for a probe wavelength of 589 nm reveals the presence of an isobestic point between K-590 and its photoproduct, which absorbs to the blue of K-590 (see text). The change in ΔA caused by pump 2, relative to ΔA without pump 2, is designated as δ. The values of δ can be both positive and negative. See text for a more detailed description.

this time interval, as previously observed.[16,22,56] This result is consistent with picosecond time-resolved vibrational data.[16,22]

Kinetic fits (solid lines, Figure 3) to PTA data at <100 ps (recorded with 1-ps resolution) are obtained from a simple mechanism describing the forward RT/BR reactions (Figure 2). The PTA data from 150 ps to 4.5 ns are recorded with 50-ps time resolution. Analogous PTA traces for probe wavelengths at 585, 592, 599, 606, and 620 nm fit the same kinetic model (data not shown).

2. K-590 Back Reaction. The photochemistry of K-590 can be experimentally distinguished from that of BR-570, even from the reactive mixtures of species found in the RT/BR photocycle, if K-590 is preferentially excited relative to BR-570 and if the relative photochemical yields from K-590 and BR-570 are at least comparable. The first criterion can be fulfilled with a three-pulse sequence (Figure 1B) in which the wavelength of pump 2 is preferentially absorbed by K-590 (e.g., 660 nm > 30 ps after pump 1). The increased absorbance of K-590 relative to BR-570 for wavelengths >570 nm is evident in Figure 2. Although at the outset, the relative photochemical yields from BR-570 and K-590 excitation are unknown, the results presented here (*vide infra*) demonstrate that they are comparable, thereby fulfilling the second criterion. Thus, although photochemistry from both BR-570 and K-590 is initiated by pump 2, these PTA experiments are designed to distinguish K-590 photochemistry, namely, to identify the K-590 photoproduct(s) and to characterize the mechanism by which it is (they are) formed following pump 2 excitation of K-590. It is also important to note that all excitation used here is shown experimentally to be in a linear range.

Experimentally, the K-590 back reaction is initiated by a second laser pulse (4.5 ps fwhm at 660 nm, pump 2) that is preferentially (relative to BR-570) absorbed by K-590. The time course of the K-590 back reaction is measured by delaying pump 2 100 ps after pump 1 and scanning the probe pulse over the −50 ps to 4.5 ns interval (Figure 2B). The 100-ps delay ensures that only BR-570 and K-590 are excited as the wavelength of the probe pulse is varied from 570 to 620 nm.

The resultant PTA traces (Figure 3) exhibit changes in ΔA directly attributable to pump 2 (Figure 3). For example, immediately after pump 2, a decrease in ΔA is observed for a 620-nm probe, whereas an increase in ΔA is observed for a 570-nm probe. For a 589-nm probe, no significant change in ΔA appears after the CCT. These changes in ΔA remain the same for the 4.5 ns interval measured (Figure 3). The initial perturbations of the ΔA traces caused by pump 2 during the CCT are not analyzed via the kinetic model described here, except to note the absence of any ΔA change that can be assigned to species analagous to J-625 (e.g., 620-nm trace, Figure 3).

Independent of a specific kinetic model, these PTA data themselves provide qualitative insight into the K-590 photoproduct, which (i) absorbs to the blue of K-590, (ii) forms without a transient J-like intermediate, and (iii) has a 589-nm isobestic point with K-590. These characteristics suggests that the K-590 photoproduct is BR-570, *vide infra*.

The influence of pump 2 by itself on the forward RT/BR photocycle is examined by substituting it for pump 1 in a two-pulse sequence (Figure 1A). Although the amount of BR-570 converted into K-590 is small (<5%) (lower BR-570 absorption coefficient at 660 nm), the kinetic fit remains the same as that used for a pump 1 of 578 nm, *vide supra*. Thus, no new BR-570 photochemistry is created by 660-nm excitation in the absence of K-590.

3. Spectral Signature of the K-590 Photoproduct. The three-pulse sequence (Figure 1B) can be extended to obtain the spectral signature of the K-590 photoproduct by measuring changes in ΔA induced by pump 2 as a function of the probe pulse wavelength. The changes in ΔA for a given probe pulse wavelength (e.g., 620 nm, Figure 3) are measured as differences between ΔA values before and after pump 2 (quantity δ in Figure 3). These δ values remain unchanged over the entire 4.5-ns time interval following pump 2 measured here (Figure 3).

The dependence of these δ values on the wavelength of the probe pulse characterizes the spectral signature of the K-590 photoproduct. The δ values are obtained by scanning the probe pulse from −50 ps to 4.5 ns using eight probe pulse wavelengths between 570 nm to 620 nm, three of which are presented in Figure 3. All of the PTA data measured with these eight probe wavelengths (570, 585, 592, 599, 605, 606, 613, and 620 nm) show that the K-590 photoproduct absorbs to the blue of K-590 and that the photoproduct and K-590 share an isobestic absorption point at 589 nm, thereby again suggesting its identification as BR-570.

A quantitative evaluation of this hypothesis can be obtained if the wavelength dependence of these δ values is compared with the absorption properties of BR-570. If the excitation of K-590 generates only BR-570, then the measured δ values created by pump 2 should quantitatively correlate with the ΔA data measured for the forward BR reaction in which only K-590 is created from BR-570 (>30 ps after excitation).

The ΔA values (570−620 nm) observed by PTA for the forward BR photocycle (Figure 3, <100 ps) can be fit well with a function obtained by comparing the BR-570 and K-590 absorption coefficients (Figure 2). Thus, the PTA data presented in this study correspond closely to the results obtained in numerous earlier studies.[7−9,52] This fit is plotted in terms of ΔA versus the probe pulse wavelength (Figure 4) and shows the change in ΔA expected if only K-590 is formed from BR-

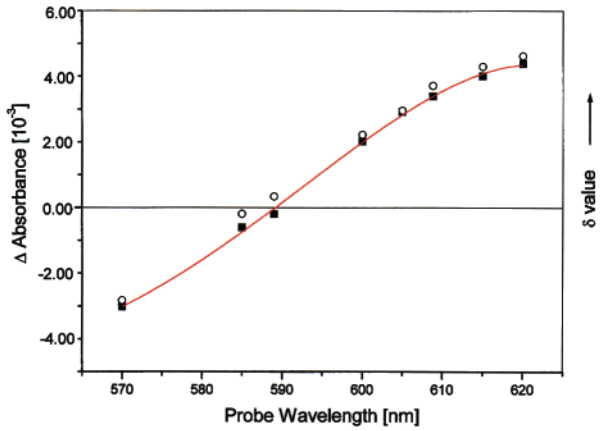

Figure 4. Scaled (see text) value of δ (Figure 2) plotted against the probe wavelength using the three-pulse sequence described in Figure 1B. These δ values measure the change in ΔA induced by pump 2 relative to the absorption spectrum of K-590. The differences in the absorbance (ΔA) that can be assigned to BR-570 and K-590 (○ data) as a function of wavelength (Figure 2B) are plotted for comparison. If these two sets of values are normalized with respect to both amplitudes and signs, their excellent agreement strongly suggests that the product of K-590 photochemistry is BR-570.

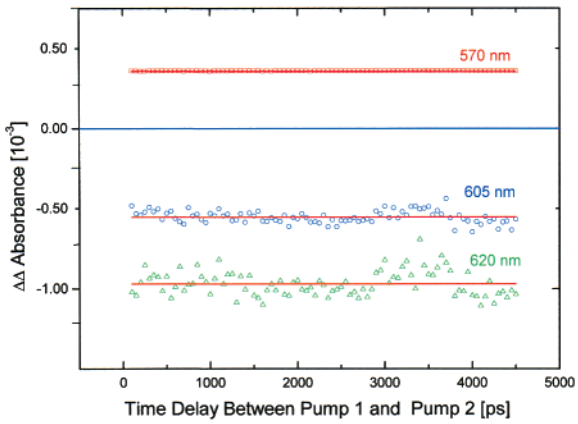

Figure 5. PTA traces measured using the three-pulse sequence described in Figure 1C. The time delay between pump 2 (570, 605, and 620 nm) and pump 1 is varied (50 ps to 4.5 ns), while the probe pulse remains at a 5.0-ns time delay. The generally constant ΔA signal recorded for all three probe pulse wavelengths indicates that the photochemistry initiated by the excitation of K-590 by pump 2 remains unchanged throughout the 50 ps to 4.5 ns interval of the K-590 lifetime monitored

570. Thus, to obtain a model for the formation of BR-570 from K-590, only the sign of the change in ΔA must be reversed. To compare the results from the three-pulse experiments presented here, therefore, the signs of the δ values are reversed and their magnitudes are scaled to account for the differences in BR-570 and K-590 concentration at 30 ps to 4.5 ns (factor of 5).

The resultant plot of the δ values versus probe pulse wavelengths is in excellent agreement with the corresponding ΔA plot obtained for the forward BR photocycle reaction (Figure 4). Not only do the ΔA and δ data have the same general wavelength-dependent shape, but the same isobestic point is also obtained. Because such excellent ΔA and δ agreement is found for all the probe pulse time delays following pump 2 (15 ps to 4.5 ns) measured, the K-590 photoproduct is stable over at least this time interval. All of these results strongly support the conclusion that the K-590 photoproduct is BR-570.

To avoid any secondary photochemistry or saturation effects, these ΔA measurements were performed in the linear power regime for pump 1 (<2.5 mW) and pump 2 (<80 mW), as determined by a series of power-dependent experiments (data not shown). The pulse power values typically used were 2.5 mW for pump 1 and 25 mW for pump 2. Static absorption spectra of the BR samples taken before and after these PTA experiments exhibited no changes.

4. Time Evolution of K-590 Photochemistry. Because K-590 is an intermediate in the BR photocycle, its photochemistry might be anticipated to change as a function of time after its formation. Such time-dependent photochemistry from a RT/BR intermediate could derive from structural changes in the retinal itself and/or from alterations of the related retinal/protein interactions or both. For example, it has been suggested from transient absorption data that K-590 forms an intermediate denoted as KL (formation times ranging from 80 ps[14] to 20 ns[57]). Although other transient absorption data[56] and time-resolved vibrational spectroscopic studies[16] found no evidence for a KL intermediate, the time evolution of K-590, and thereby the potential appearance of KL, is examined independently by the multiple-pump experiments described here.

A three-pulse sequence is used to examine this issue by fixing pump 1 (0 ps) and the probe pulse (4.5 ns) in time while pump 2 is scanned from 50 ps to 4.5 ns (Figure 1C). Because the probe pulse monitors the net photochemical change (i.e., forward versus back reactions), variations in the K-590 photochemistry appear as different ΔA probe pulse signals. No ΔA changes are observed over the entire 50 ps to 4.5 ns interval scanned by pump 2, as illustrated in Figure 5 for a 605-nm probe wavelength. Analogous ΔA data taken for probe wavelengths of 570, 585, 592, 599, 606, 613, and 620 nm also exhibited no change in the 50 ps to 4.5 ns interval (data not shown). Collectively, these data demonstrate that the photochemical properties (photoproduct and relative yield) of K-590 over the 50 ps to 4.5 ns time interval of the BR photocycle do not change.

Discussion

Although the existence of photoreactions initiated from the intermediates constituting the RT/BR photocycle (i.e., back reactions) has been established in a variety of studies utilizing different techniques and experimental conditions (including LT trapping),[46−49] the back reaction originating from the excitation of K-590 has not been characterized previously in detail. The K-590 back reaction is especially interesting mechanistically, as it involves retinal isomerization that is the reverse of that occurring in the forward RT/BR photocycle. Specifically, a variety of spectroscopic data, including time-resolved vibrational spectra of K-590,[13−15] have shown that BR-570 contains an all-*trans* retinal, whereas K-590 contains a 13-*cis* retinal. Thus, the forward RT/BR photocycle involves *trans* to *cis* isomerization at the C_{13}═C_{14} bond, whereas the K-590 photoreaction involves the reverse *cis* to *trans* isomerization at the same bond.

Earlier studies did not experimentally distinguish the back reaction from a specific BR intermediate because (i) the wavelengths used to initiate the back reaction(s) are absorbed by more than one BR intermediate, (ii) the duration of the back reaction excitation overlapped the kinetic lifetimes of multiple BR intermediates, or (iii) both.[24,28] Thus, these earlier experiments created photostationary-state mixtures of ground and excited electronic state populations from a variety of BR intermediates, at least some of which initiated photolytic back reactions. The composition of these mixtures depends strongly on the experimental parameters (pulse width, energy, wavelength, etc.) selected as well as the chemical (e.g., pH and temperature) conditions of the sample. Undoubtedly, the pres-

ence of more than one back reaction also complicates both the measurement of time-resolved spectroscopic data and its detailed interpretation.

Other studies have relied on thermally trapping reactive BR species at LT, after which, back reactions are photolytically initiated from the stable, frozen sample, and the resultant products analyzed at either LT or RT .[46−49] Given the recognized influence of the protein environment, and especially that part forming the protein binding pocket for the retinal chromophore, it is unlikely that conclusions concerning the RT reaction dynamics can be derived directly from LT data for two reasons: (i) the retinal/protein interactions are almost certainly different at LT than at RT because the RT photocycle is effectively interrupted at LT (presumably by altering these retinal/protein interactions), and (ii) there is no *a priori* reason to conclude that the LT sample is homogeneous (e.g., composed of only a single, pure BR intermediate). Thus, back reaction originating from a single intermediate in the RT/BR photocycle can be characterized most accurately from RT, time-resolved measurements of the type presented here.

LT experiments show that the K → BR photoreaction proceeds with a quantum yield of ∼1 at −165 °C (∼1.5 times the BR → K yield at LT versus ∼1.6 times the BR → K yield at RT[29,30]). This quantum yield is wavelength-independent at 77K.[29,31] As in the case of the forward BR photocycle, the quantum yield for the reverse K → BR photoreaction is essentially temperature-independent,[29,39] although at 13 K, the reverse K → BR photoreaction is faster than the forward K → BR photoreaction.[42] Because the sum of the quantum yields is greater than one for the reverse and forward photoreactions, photoexcitation of K-590 and BR-590 cannot populate a common excited electronic state. In addition, the absence of a temperature dependence suggests that the photoinduced conversion of K → BR involves a barrierless process. In all of the LT experiments reported, shifted absorption maxima (e.g., 5 nm for BR-570 and 20 nm for K-590 at 90 K) are interpreted in terms of a heterogeneous BR sample (e.g., conformers of K-590 and BR-570). These distinct conformational forms become equilibrated at 200 K. The LT heterogeneity extends to the retinal protein environment and can be manifested as variations in the distances between the retinal and charged amino acids residues and water molecules constituting the surrounding protein structure.[29]

Three major conclusions concerning the K → BR photoreaction can be reached from the data presented here: (i) excitation of K-590 over the 650−660-nm region initiates the formation of BR-570 within the 5-ps duration of the excitation pulse, (ii) the K-590 to BR-570 back reaction remains unchanged throughout the 50 ps to 4.5 ns lifetime of K-590, and (iii) no intermediate (e.g., analogous to J-625 in the BR-570 forward reaction) is observed between K-590 and BR-570.

The <5-ps isomerization from 13-*cis* to all-*trans* retinal generated by photoexcitation of K-590 contrasts with the long (5-ms) conversion that occurs at the end of the thermal RT/BR photocycle (i.e., O-640 to BR-570[58]), and therefore, the photoinduced and thermal isomerizations appear to proceed by two different molecular mechanisms.

The observation that the K-590 photochemistry is unchanged throughout the 50 ps to 4.5 ns period of its lifetime is consistent with the PTR/CARS data reported previously,[16] which show that the retinal structure in K-590 also remains unchanged over this same time interval. Because the retinal structure is unchanged, its mechanistic role in the K-590 back reaction must also remain unchanged. By implication, the other major components of the mechanism, the structure of the protein binding pocket and its retinal/protein interactions, also remain unchanged during the 50 ps to 4.5 ns period.

This last observation suggests that the mechanism for K-590 to BR-570 photoconversion is significantly different from that of BR-570 to K-590 forward reaction. In the latter case, BR-570 excitation populates Franck−Condon levels in BR*-570, which undergo dephasing (200−500 fs) prior to the formation of J-625, which subsequently (3.5 ps) decays to K-590.[14,53] Recent vibrational spectra of J-625, measured by picosecond time-resolved coherent anti-Stokes Raman scattering (PTR/CARS),[15,59] demonstrate that the retinal in J-625 remains all-*trans* and that C_{13}═C_{14} retinal isomerization occurs as J-625 transforms into K-590 (13-*cis*) and not prior to J-625, as previously proposed.[4−6,15,59] These same PTR/CARS data show that J-625 contains a distinct retinal structure relative to both BR-570 and K-590.[59] Thus, the forward reaction utilizes the J-625 (both its retinal structure and the associated retinal/protein interactions) as a precursor to C_{13}═C_{14} isomerization.

Recent interpretations of PTR/CARS data also suggest that J-625 is an excited electronic state.[59] In such a case, the properties of J-625 that facilitate all-*trans* to 13-*cis* retinal isomerization in the BR photocycle would include electronic state properties (e.g., electronic symmetries that control state crossings). As already noted, this mechanistic interpretation focuses on the role of the retinal binding pocket and its retinal/protein interactions on C_{13}═C_{14} isomerization.

Because PTA data (Figure 3) show that no intermediate analogous to J-625 is present in the K-590 back reaction (PTA measurements on the forward photocycle detect J-625 with its 200-fs formation and 3.5-ps decay times[6−10]), the protein binding pocket and the retinal/protein interactions present during the 50 ps to 4.5 ns lifetime of K-590 must facilitate C_{13}═C_{14} isomerization and, therefore, the formation of BR-570. There appears to be no need to form a J-like intermediate in the K-590 back reaction. Thus, the mechanisms of the forward BR photocycle and the K-590 back reaction are different.

For the K-590 back reaction, optical excitation of K-590 populates Franck−Condon levels in its excited electronic state (K*-590), which forms BR-570 directly within 5 ps. The protein binding pocket and retinal/protein interactions present in K*-590 facilitate C_{13}═C_{14} isomerization without the need to form another intermediate (e.g., a J-like species). These structural conditions remain unchanged throughout the 50 ps to 4.5 ns lifetime of K-590 examined here.

The absence of a J-like species in the K-590 back reaction can be viewed mechanistically in terms of the protein binding pocket and its retinal/protein interactions that facilitate C_{13}═C_{14} isomerization. Obviously, they are either the same or different for all-*trans* to 13-*cis* versus 13-*cis* to all-*trans* isomerization. The observation that the K-590 back-reaction mechanism remains unchanged for 2 orders of magnitude in time suggests that the former case holds. Namely, once the configuration of the protein binding pocket and its retinal/protein interactions are arranged to facilitate the all-*trans* to 13-*cis* transformation in BR-570, the isomerization process can be reversed without a need to alter the protein binding pocket or its retinal/protein interactions. Thus, the appearance of J-625 represents a unique channel through which the forward reaction must pass, but which is not required by the K-590 back reaction.

Finally, it should also be noted that the distinct photochemistry of K-590 relative to that of BR-570 indicates that the excited electronic state potential surface represented by K*-590 is not directly connected to that of BR*-570. There is no

experimental evidence presented here to support the view expressed in the interpretation of earlier results[60] that K-590 and BR-570 share an excited electronic state potential surface.

Acknowledgment. This research was supported by Grant MCB 9245844 from the Biophysics section of the National Science Foundation.

References and Notes

(1) Oesterhelt, D.; Stoeckenius, W. *Nat. New Biol.* **1971**, *233*, 149−152.
(2) Racker, D. D.; Stoeckenius, W. *J. Biol. Chem.* **1974**, *249*, 662−663.
(3) Ottolenghi, M. *Methods Enzymol.* **1982**, *88*, 470−491.
(4) Birge, R. R. *Biochim. Biophys. Acta* **1990**, *1016*, 293−327.
(5) Lanyi, J. *J. Struct. Biol.* **1998**, *124*, 164.
(6) Mathies, R. A.; Lin, S. W.; Ames. J. B.; Pollard, W. T. *Annu. Rev. Biophys. Chem.* **1991**, *201*, 491−518.
(7) Nuss, M.; Zinth, W.; Kaiser, W. Killing, E.; Oesterhelt, D. *Chem. Phys. Lett.* **1985**, *117*, 1−7.
(8) Pollard, H.-J.; Franz, M. A.; Zinth, W.; Kaiser, W.; Killing, E.; Oesterhelt, D. *Biophys. J.* **1986**, *49*, 651−662.
(9) Patrick, J. W.; Breton, J.; Martin, J. L.; Antoinette, A. *Chem. Phys. Lett.* **1987**, *137*, 369−375.
(10) Doble, J.; Zinth, W.; Kaiser, W.; Oesterhelt, D. *Chem Phys. Lett.* **1988**, *144*, 215−220.
(11) Terner, J.; Hseih, C.-L.; Burns, A. R.; El-Sayed, M. A. *Proc. Natl. Acad. Sci. U.S.A.* **1974**, *76*, 3046.
(12) Stockberger, M.; Klusmann, H.; Gattermann, G.; Massif, G.; Peters, R. *Biochemistry* **1979**, *18*, 4886−4990.
(13) Brack, T. L.; Atkinson, G. H. *J. Mol. Struct.* **1989**, *214*, 289−303.
(14) Doig, S. J.; Reid, P. J.; Mathies, R. A. *J. Phys. Chem.* **1991**, *95*, 6372−6379.
(15) Ujj, L.; Jäger, F.; Popp, A.; Atkinson, G. H. *Chem. Phys.* **1996**, *212*, 421−436.
(16) Weidlich, O.; Ujj, L.; Jäger, F.; Atkinson, G. H. *Biophys. J.* **1997**, *72*, 2329−2341.
(17) Song, Li.; El-Sayed, M. A. *J. Am. Chem. Soc.* **1998**, *120*, 8889−8890.
(18) Gerwert, K.; Souvignier, G.; Hess, B. *Proc. Natl. Acad. Sci. U.S.A.* **1990**, *87*, 9774−9778.
(19) Braiman, M. S.; Bousche, O.; Rothschild, K. *J. Proc. Natl. Acad. Sci. U.S.A.* **1991**, *88*, 2388−2392.
(20) Noelker, K.; Weidlich, O.; Siebert, *F. Springer Proc. Phys. (Time-Resolved Vib. Spectrosc. V)* **1992**, *68*, 57−60.
(21) Hage, W.; Kim, M.; Frei, H.; Mathies, R. A. *J. Phys. Chem.* **1996**, *100*, 16026−16033.
(22) Dioumaev, A. K.; Braiman, M. S. *J. Phys. Chem.* **1997**, *101*, 1655−1662.
(23) Gerwert, K. *Biol. Chem.* **1999**, *380*, 931−935
(24) Goldschmidt, C. T.; Ottolenghi, M.; Korenstein, R. *Biophys. J.* **1976**, *16*, 839−843.
(25) Balashov, S. P.; Litvin, F. F. *Biophysics* **1981**, *26*, 566.
(26) Grieger, I.; Atkinson, G. H. *Biochemistry* **1985**, *24*, 5660−5665.
(27) Ames, J. B.; Mathies, R. A. *Biochemistry* **1990**, *29*, 7181−7190.
(28) Govingdjee, S. P.; Balashov, S. P.; Ebrey, T. G. *Biophys. J.* **1990**, *58*, 597−843.
(29) Balashov, S. P.; Imasheva, E. S.; Govindjee, R.; Ebrey, T. G. *Photochem. Photobiol.* **1991**, *54*, 955−961.
(30) Bazhenov, V.; Schmidt, P.; Atkinson, G. H. *Biophys. J.* **1992**, *61*, 1630−1637.
(31) Balashov, S. P. *Isr. J. Chem.* **1995**, *35*, 415−428.
(32) Eisfeld, W.; Pusch, C.; Diller, R.; Lohrmann, R.; Stockburger, M. *Biochemistry* **1993**, *32*, 7196−7215.
(33) Edman, K.; Nollert, P.; Royant, A.; Belrhali, H.; Pebay-Peyroula, E.; Hajdu, J.; Neutze, R.; Landau, E. M. *Nature* **1999**, *401*, 822−826.
(34) Subramaniam, S.; Gerstein, M.; Oesterhelt, D.; Henderson, R. *EMBO J.* **1993**, *12*, 1−8.
(35) Dioumaev, A. K.; Brown, L. S.; Needleman, R.; Lanyi, J. K. *Biochemistry* **1998**, *37*, 9889−9893.
(36) Luecke, H.; Schobert, B.; Richter, H. T.; Cartailler, J. P.; Lanyi, J. K. *Science* **1999**, *286*, 255−260.
(37) Litvin, F. F.; Balashov, S. P.; Sineshchekov, V. A. *Bioorg. Khim.* **1975**, *1*, 1767−1777.
(38) Balashov, S. P.; Litvin, F. F. *Bioorg. Khim.* **1976**, *2*, 565−566.
(39) Hurley, J. B.; Ebrey, T. G.; Hong, B.; Ottolenghi, M. *Nature* **1977**, *270*, 540−542.
(40) Lozier, R. H.; Niederberger, W. *Fed. Proc.* **1977**, *36*, 1805−1809.
(41) Kalisky, O.; Lachish, U.; Ottolenghi, M. *Photochem. Photobiol.* **1978**, *28*, 261−263.
(42) Kryukov, P. G.; Matveets, Yu. A.; Sharkov, A. V.; Lasarev, Yu. A.; Terpugov, E. L. *Springer Ser. Opt. Sci (Lasers Photomed. Photobiol.)* **1980**, *22*, 200−206.
(43) Xie, A. *Biophys. J.* **1990**, *58*, 1127−1132.
(44) Litvin, F. F.; Balashov, S. P. I *Biophysics* **1977**, *22*, 1111.
(45) Hurley, J. B.; Becher, J. B.; Ebrey, T. G. *Nature* **1978**, *272*, 87.
(46) Iwasa, T.; Tokunaga, F.; Yoshizawa, T.; Ebrey, T. G. *Photochem. Photobiol.* **1980**, *31*, 83−85.
(47) Birge, R. R.; Cooper, T. M.; Lawrence, A. F.; Masthay, M. B.; Vasilakis, C.; Zhang, C. F.; Zidovetzki, R. *J. Am. Chem. Soc.* **1989**, *111*, 4063−4074.
(48) Balashov, S. P.; Karneeva, N. V.; Litvin, F. F. *Biol. Membr.* **1990**, *7*, 586−592.
(49) Balashov, S. P.; Imasheva, E. S.; Govindjee, R.; Ebrey, T. G. *Photochem. Photobiol.* **1991**, *54*, 955−961.
(50) Atkinson, G. H.; Brack, T. L.; Blanchard, D.; Rumbles, G. *Biophys. J.* **1989**, *55*, 263−274.
(51) Atkinson, G. H; Blanchard, D.; Brack, T. L. *J. Lumin.* **1991**, *48 & 49*, 410−414.
(52) Blanchard, D.; Gilmore, D. A.; Brack, T. L.; Lemaire, H. Atkinson, G. H. *Chem. Phys.* **1991**, *154*, 155−170.
(53) Gai, F.; Hasson, K. C.; McDonald, J.; Anfinrud, P. A. *Science* **1998**, *279*, 1886−1891.
(54) Oesterhelt, D.; Stoeckenius, W. *Methods Enzymol.* **1974**, *31*, 667−671.
(55) Pasternak, C.; Corda, D.; Stieve, H.; Shinitzky, M. *Ann. N.Y. Acad. Sci. (Lumin. Biol. Synth. Macromol.)* **1981**, *366*, 265−273.
(56) Delaney, J. K.; Brack, T. L.; Atkinson, G. H. *Biophys. J.* **1993**, *64*, 1512-1519.
(57) Milder, S. J.; Klieger, D. S. *Biophys. J.* **1988**, *53*, 465−468.
(58) Smith, S. O.; Pardoen, J. A.; Mulder, P. P. J.; Curry, B.; Lugtenburg, J.; Mathies, R. *Biochemistry* **1983**, *22*, 6141.
(59) Atkinson, G. H.; Ujj, L.; Zhou, Y. *J. Phys. Chem.* **2000**, *104*, 4130−4139.
(60) Haupts, H.; Tittor, J.; Oesterhelt, D. *Annu. Rev. Biophys. Biomol. Struct.* **1999**, *28*, 367−399.